

Promoting of Biomechanics' Properties Incisional Wound Repair by Mesenchymal Stem Cell Transplantation

Maryam Habibi¹, Jafar Rezaian², Pooria Ali³, Rasool Mohammadi⁴, Hassan Ahmadvand⁵, Abolfazl Abaszadeh⁶, Farzaneh Chehelcheraghi^{7*}

1. Student Research Committee, School of Medicine, Lorestan University of Medical Sciences, Khorramabad, Iran
2. Department of Anatomical Sciences, School of Medicine, Lorestan University of Medical Sciences, Khorramabad, Iran
3. Department of Cardiology, School of Medicine, Shahid Madani Hospital Lorestan University of Medical Sciences, Khorramabad, Iran
4. Department of Biostatistics and Epidemiology, School of Health and Nutrition, Nutritional Health Research Center, Mehr Psychiatric Hospital, Shahid Madani Hospital Lorestan University of Medical Sciences, Khorramabad, Iran
5. Clinical Biochemistry Molecular Research Center, Institute of Mental Health and Addiction Hamadan University of Medical Sciences, Hamadan, Iran
6. Department of Plastic and Reconstructive surgery, School of Medicine, Iran University of Medical Sciences, Tehran, Iran
7. Medical Ethics and Law Research Center, Research Institute of Functional Neurosurgery, Shahid Beheshti University of Medical Sciences, Tehran, Iran

*Corresponding Author:

Farzaneh Chehelcheraghi

Medical Ethics and Law Research Center, Research Institute of Functional Neurosurgery, Shahid Beheshti University of Medical Sciences, Tehran, Iran

Email: fr.chehelcheraghi@gmail.com

Received: ***

Accepted: ***

ABSTRACT

Background: Diabetes mellitus is related to wound healing process impairments and molecular abnormalities of the wound. We aimed to evaluate the therapeutic potential of semi-solid bone marrow as a source of stem cells (SCs) in regenerative medicine.

Methods: This trial study was conducted at the Faculty of Medicine, Lorestan University of Medical Sciences, Khorram Abad, IRAN in 2019. Forty five Albino Wistar rats with an average weight of 250–300g, were purchased from Lorestan Aftabavaran Company in (Khorramabad, Lorestan, Iran). The rats were divided into 3 groups (n=15). For all groups, Streptozotocin (STZ) (Single dosage; 65 mg/kg, i.p.) was used to induce diabetes, and Sharp dissection was used to draw and pull down a dorsal skin flap (9×3 cm) in the control and saline groups on day0, respectively. The group used 7×10^9 BMMSCs on day 0. Histologic specimens were stained with hematoxylin and eosin and were stained with trichrome mason. Biomechanic measurements were taken in the wound area.

Results: The epidermal thickness was increasing and blood vessels were growing. In the cells group, hair follicle destruction, cellular penetration, diffuse fibrosis, and necrosis were not observed in comparison with the saline and control groups. The Cells group had a higher energy absorption than the Bending stiffness and Maximal Force Ultimate Tensile Strength (UTS) group on day 14 as a result of decreased Bending stiffness and Maximal Force Ultimate Tensile Strength (UTS).

Conclusion: According on result of recent study, Stem cells can improve the healing of diabetic incision wounds.

KEYWORDS

Streptozocin; Tensile Strength; Bone Marrow; Biomechanical Phenomena; Regenerative Medicine; Wound Healing; Collagen; Mesenchymal Stem Cells; Necrosis; Diabetes Mellitus

Please cite this paper as:

Habibi M, Rezaian J, Ali P, Mohammadi R, Ahmadvand H, Abaszadeh A, Chehelcheraghi F. Promoting of Biomechanics' Properties Incisional Wound Repair by Mesenchymal Stem Cell Transplantation. World J Plast Surg. 2025;14(2):1-9.

doi: 10.61186/wjps.14.2.**

INTRODUCTION

The importance of wound healing lies in ensuring the skin's anatomic integrity and its functional structure. When the integumentary system repairs itself after an injury, wounds are formed. The healing process of the skin and other soft tissues is what causes wounds^{1, 2}. During these phases, the wound healing process can be interrupted by aberrancies, and prolongations that could occur, finally cause persistent wounds that fail to heal. The most common complications of Diabetes Mellitus (DM) are altered wound healing. Major chronic complications are caused by the deterioration of the wound healing process in diabetic patients as a result of hyperglycemic conditions³. An excessive inflammatory, deferred generation and remodeling responses are part of the multifactorial mechanism that causes delayed wound healing⁴. The process of diabetic wound healing involves releasing pro-inflammatory cytokines like IL-1 β , IL-6, and TNF- α . High blood glucose has been associated with hindered cell proliferation in diabetic patients, as shown by numerous studies. The growth factor and collagen production were decreased during wound healing. The lack of VEGF and TGF-1 growth factors in diabetics can lead to impaired wound healing as a result of reduced angiogenesis⁵⁻⁷. Skin is a tissue that is constantly evolving as we age and are influenced by gender. Biomechanical tensile testing, which involves stretching tissue and developing a force, has provided us with much of our current understanding of skin behavior. Despite the fact that failure properties have typically been the focus of previous tensile analyses, recent research has focused on the relevance of skin's viscoelastic behavior at low loads to normal physiological functioning. The skin's capacity to resist elongation, carry weight, and dissipate energy through a viscous method can be identified when these biomechanical properties are understood⁸. The plane of skin and scar can be studied in mutual orthogonal directions. The directionality of healthy tissue can be viewed through these measures, and the directional properties undergo changes as a result of injury⁹. The differences in biomechanical properties between skin and scar tissue indicate that there may be morphological changes that can occur following injury, as demonstrated by the viscoelastic and directional changes observed. The

considerably compromised biomechanical function and decreased failure resistance of the need for clinical treatments to restore normal viscoelastic behavior to the wound site. The healed wound will have better functionality and aesthetics due to increased tension compatibility between coverings and reduced scratching. Structural adaptation to loading occurs in both skin and scar tissue, with collagen rapidly realigning parallel to stretch¹⁰. Clinical and preclinical data¹¹, indicate that there is pronounced scarring in anatomical areas with high tissue tension. The wound environment's biomechanics can have a major impact on healing outcomes. The use of a force-modulating polymer wound dressing has shown that reducing tension in healing wounds could reduce scarring significantly¹². Stem cells (SCs) are believed to have the ability to divide indefinitely and produce more differentiated progeny in general¹³. This process usually starts from transient amplifying cells (i.e., relatively undifferentiated cells with exceptionally high proliferative potential, but limited cell cycles that can be traversed), whose progeny then generates and regenerates tissues. Enhancing the expression levels of vascular endothelial growth factor (VEGF) can be achieved with various stem cell types to improve chronic diabetic wounds, initiating the growth of cells, angiogenesis, and granulation tissue creation in traumatic tissue^{14, 15}.

We aimed to examine the impact of SS on wound healing through histochemical and biomechanical methods.

MATERIALS AND METHODS

The process of separating and purifying BM-MSCs

BM-MSCs were extracted from healthy 1-week-old Albino Wistar rats. Primary cells were obtained as described in our previous research, (24) and cultured in LG-DMEM supplemented with 1% (W/V) penicillin-streptomycin in the atmosphere of 37 °C and 5% CO₂. When the cells reached ~80% confluence, the adherent cells were digested with 3ml 0.25% (W/V) trypsin/EDTA at 37 °C for 3 min and then passaged. Three to four passages of BM-MSCs were used for the following experiments that were confirmed in the Iranian biological resource center. BMMSCs were also labeled with fluorescence molecule (DiI cell-labeling solution)¹⁶.

Animal studies

The study utilized 45 Wistar-Albino rats that weighed 200–220 g. Permission Number and ethical code: IR.LUMS.REC.1397.111.

All animals were given the same standard conditions. Intraperitoneal injection of STZ (65mg/kg) was used to prepare diabetic rat models. The DM model was considered successful if the blood glucose level exceeded 16.7mmol/Lat within 1 week after the STZ injection. The study lasted for time when blood glucose levels were recorded. Three groups of rats were randomly divided, with 15 rats per group. The control-operated group did not receive any treatment. The saline-operated and BM-MSCs groups were both treated with sharp dissection to draw and pull up a dorsal skin flap (9×3 cm). No treatment was given to the Control group. Normal saline was applied to the injury area by the saline group. An application of a cell containing 6×10^9 was made to the incision region of the BM-MSCs group. From day 0, all cells were applied to animals every day.

Incision wound model

Before and during the experimental interventions, all animals were administered anesthesia. Before the experimental wounds were inflicted, the rats had their dorsal skin shaved. Under sterile conditions, the surgical interventions were performed with anesthesia administered intravenously using ketamine (75 mg/kg) and xylazine (8 mg/kg). Ersel talked about making and taking out a lateral skin flap that measures 9×3 cm (27 cm²) on the lateral side of rats ¹⁷. The flap was degraded so much that it fell below the panniculus carnosus level. The incisions were closed with a surgical suture made of silk that is 1 cm away from the divided animal coating. The wounds were not covered. Each rat was given a full 15-minute period.

Wound healing

The flap viability was assessed on the 7th and 14th day after the initial surgery. The operationability of flap skins was assessed by rats on the 7th and 14th postoperative days. The epidermal thickness and necrotic area were determined by taking five separate measurements in each slice, through six

slices being arbitrarily designated as of animal in a group. The dorsal skin flaps were captured. To define the necrotic skin surface, the borders of the necrotic skin were used to calculate the percentage of necrotic tissue, and the surgical borders of the flaps were used to delimit the total flap areas. Calculating the percentage of necrotic tissue was done using the borders of the necrotic skin.

Histopathological analysis

Following the fixation of the skin biopsy samples in 10% buffered formalin for 24 hours, the samples were embedded with paraffin wax and blocked. The use of a Leica RM 2145 model microtome (Germany) for cutting around 5µm sections was followed by staining with both hematoxylin and eosin, along with Mallory azan staining. The thickness of the epithelium was examined during the investigation of sections at a magnification of 40x. After taking digital photos (Olympus BX51 Light Microscope, Olympus C5050 Digital Camera, Japan) at a magnification of 20×, necrotic skin and total flap area border were determined with the aid of a software program (ImageJ) bundled with 64-bit Java 1.8.0_172(70MB)¹⁸.

Histologic grading

The tissue collagen discoloration was graded as normal with 0; mild increase with 1; mild to moderate increase with 2; moderate increase with 3; moderate to marked increase with 4; and marked increase with 5. To express the cellular infiltration grade, the scoring was obtained by counting the total inflammatory cells (lymphocytes, neutrophils, macrophages, eosinophils, plasma cells, and mast cells) for each section per high-power field (HPF) (400×). According to this scoring, a score of 0=<3 inflammatory cells, 1=3–11 inflammatory cells, 2=11–20 inflammatory cells, 3=21–30 inflammatory cells, 4=31–40 inflammatory cells, and 5 = >41 inflammatory cells ¹⁷.

Biomechanical analysis

Standardized rectangular strips of the specimen (5 × 40 mm) were removed from across the incision and adjacent skin. The specimen was mounted in a material testing machine (Zwick Z 2–5– PH 1 F,

Germany). The deformation rate was kept constant at 15 mm/min. From the load-deformation curve, we determined the Energy Absorption (Nmm²), maximal force (N), ultimate tensile strength (N/mm²), and Bending stiffness (N/mm²)¹⁹.

Statistical analysis

The expression of data is mean \pm SD. SPSS ver. 22.0 (IBM Corp., Armonk, NY, USA) was used to perform a statistical comparison of the groups. Analysis of significant differences between groups was conducted using the Kruskal-Wallis test. The Mann-Whitney U test was utilized for post-hoc analysis after the significance was determined. The presence of a *P*-value below 0.05 was deemed to be statistically significant.

RESULTS

In Vitro cell label assessment experiments

On the seventh day after surgery, we noted that the CM-Dil-labeled BMMSCs could still be found in the region of the flaps in the BMMSCs group.

Histopathological results

The entire number of hair roots

A significant difference was found among the 3 groups (KWc2, *P*<0.001 and *P*<0.0001 respectively day 7 and day 14) (Figure 1). As a post-hoc examination, the groups were associated in pairs with the Mann-Whitney U test. We detected that there was a statistically significant difference between the Cells group and the Control operated group (*P*=0.02, *P*=0.003 respectively day 7 and day 14) and the Saline group (*P*=0.05, *P*=0.008 respectively day 7 and day 14). After 14 d, there were more hair roots in the Cells group than in the Control managed and the Saline groups.

Amount of deteriorated hair roots

The Cells group had an increase in hair roots compared to the Control operated and the Saline groups after 14 d. There was a statistically significant difference between the Cells group and the Control managed group (*P*=0.01, *P*=0.002 respectively day 7 and day 14) and the Saline group (*P*=0.01, *P*=0.002

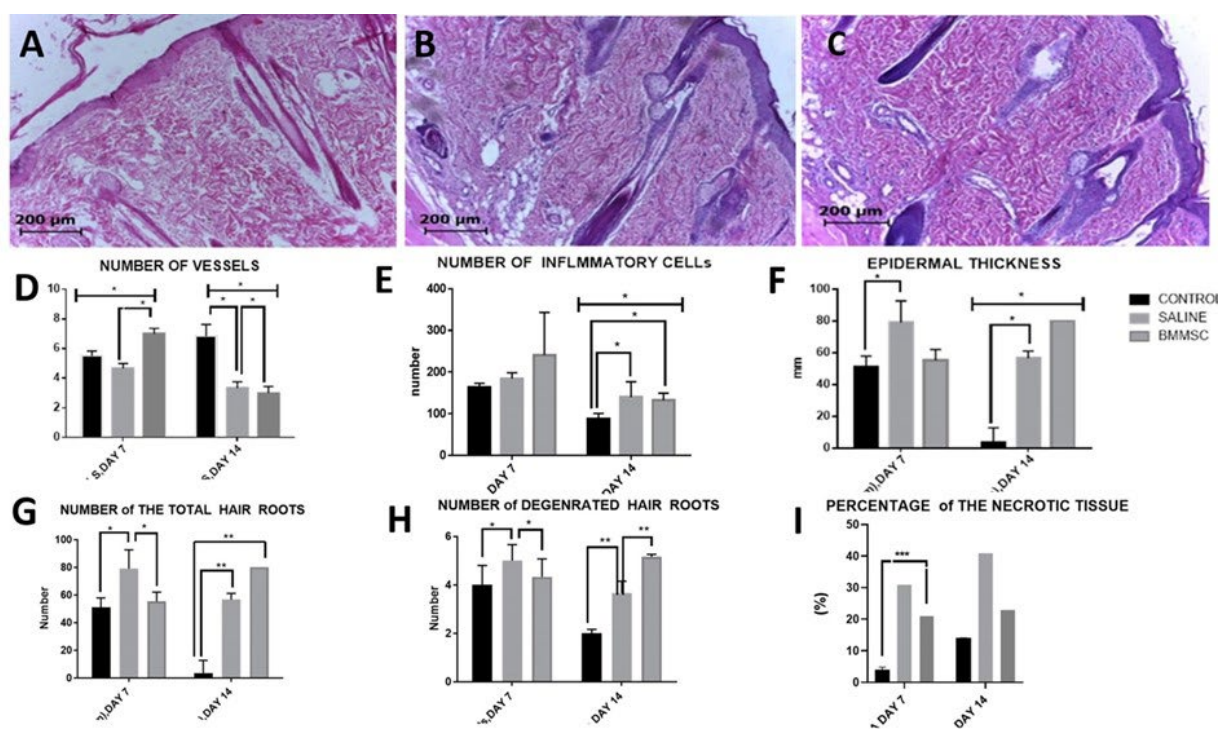


Figure 1: Light microscopic images and graphs of dorsal skin flap: (A) control group, (B) Saline group, (C) Cell group, (D) graphs of several vessels, (E) graphs of several inflammatory cells (F) epidermal thickness, (G) number of the total hair roots, (H) number of degenerated hair roots and (I) number of the necrotic tissue. H&E staining, original magnification $\times 20$, scale bar = 200 μ m

respectively day 7 and day 14) after post hoc analyses (Mann-Whitney U test). The Cells group had less degenerated hair roots on the 7th and 14th d than the Control operated and the Saline group (Figure 1).

Amount of vessels

We initiated a significant difference between completely the groups in relations of the entire amount of the vessels (KWc2, $P<0.001$, $P=0.000$ respectively day 7 and day 14). The groups were associated as sets by applying the Mann-Whitney U test as post hoc analysis, showing a statistically significant difference between the control group and the Cell group ($P=0.008$, $P=0.69$ respectively day 7 and day 14), and between the Cell group and the Saline operated group ($P=0.000$, $P=0.000$ respectively day 7 and day 14). The Cells group had a higher number of intact vessels compared to the Control operated group and the Saline group (Figure 1).

Epidermal thickness

There was a statistically no significant difference among all the groups (KWc2 $P<0.1$ 21 day 7 and

but significant on day 14 $P=0.022$) (Figure 1). The groups were associated in sets by applying the Mann-Whitney U test as a post hoc analysis. It was deceived after the comparisons that there was a statistically no significant difference between the control group and the cell group ($P=0.755$, $P=0.275$ respectively day 7 and day 14), and the between the cell group and the saline group ($P=0.05$, $P=0.002$ $P=0.067$ respectively day 7 and day 14). The epidermal thickness of the cell group was higher than that of the control operated group and saline group at the end of the 14th day.

Ratio of the necrotic tissue

Statistically, no significant differences were determined between the control group, the saline group, and the cells group in terms of the percentage of necrotic tissue in the section. Areas (KWc2, $P=0.421$) (Figure 2). The groups were associated as sets by applying the Mann-Whitney U test as a post hoc analysis, showing that the necrotic tissue ratio in the cell group was lower than in the control group ($P=0.000$, $P=0.198$ respectively day 7 and day 14). The saline group had a higher percentage of necrotic tissue than the cell group on days 7 and 14. At the

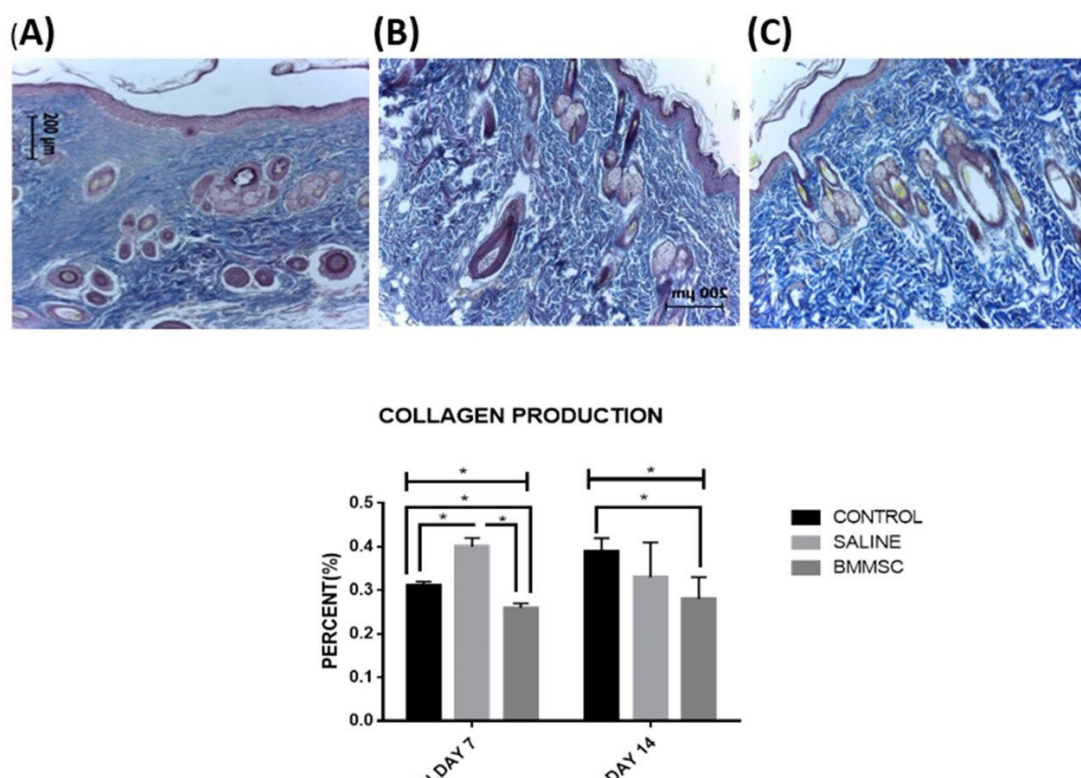


Figure 2: Trichrome Masson staining of the sections images of dorsal skin flap: (A) control group, (B) saline group, (C) BMMSC group. Original magnification $\times 20$, scale bar=200 μm

end of the 14th day, the cell operation limited the creation of necrotic tissue in the areas.

Cellular penetration

The study groups did not have any significant ($P=0.130$) differences in charges of cellular penetration grade. It was completed after the juxtaposition that there was a statistically no significant difference among the control group and the cell group on day7 ($P=0.053$), but significant on day14 ($P=0.02$), and the between the cell group and the saline group no significant on day7 ($P=0.571$), but significant on day14 $P=0.01$. A post-hoc analysis involved comparing the groups in sets applying the Mann-Whitney U exam. During the study, the penetration rates in the control group were 0–1, the penetration rates in the cell group were 1–2, and the infiltration rates in the group were 3–4. Cellular infiltration was found to be lesser in the cell group than in the saline group and the control group (Figure 1).

Diffuse fibrosis

Figure 3 displays the results of scoring the collagen production observed in the tissues of all study groups. The intact control group had a score of 0–1, while the cell group had a score of 1–2, but the scores in the control group were mostly 3–4. The saline group had higher collagen production scores than the cell group. The study groups did not have any significant differences ($P=0.130$) in terms of cellular infiltration scores. It was determined after the comparisons that there was a statistically significant difference between the control group and the cell group on day 7 ($P=0.04$), and day 14 ($P=0.019$), and the between the cell group and the saline group significant on day7 ($P=0.000$), but no sign on day 14 $P=0.221$ (Figure 3).

Biomechanical parameters

the biomechanical parameters were determined. According to these analyses on day 7, the Energy

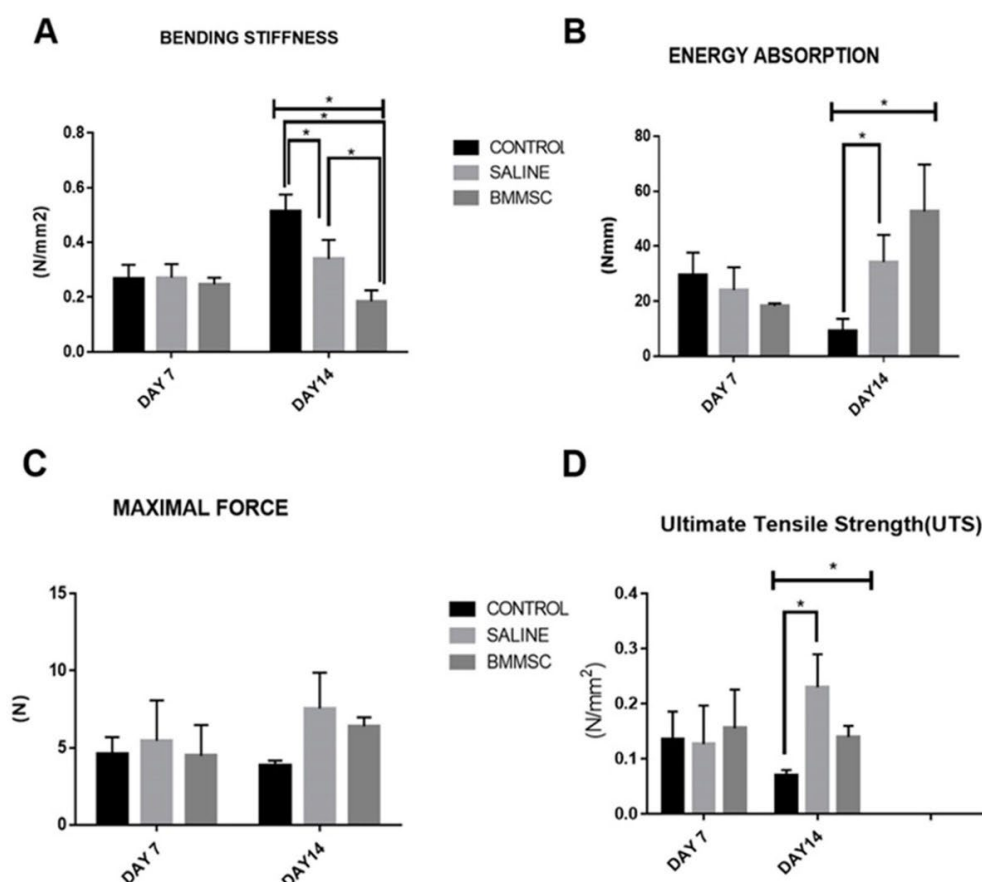


Figure 3: Comparison of Mean \pm SEM parameters of flap biomechanics in rats on days 7 and 14, respectively (A) Bending Stiffness, Energy Absorption (B), Maximal Force (C), and Ultimate Tensile Strength (UTS)

Absorption (Nmm²), maximal force (N), ultimate tensile strength (N/mm²), and Bending stiffness (N/mm²), as being no sign in the cell group between and compared in the pairs group. On day 14, only ultimate tensile strength (N/mm²), and Bending stiffness (N/mm²), as being signed in all study groups.

DISCUSSION

Wound healing is an instinctive reaction to tissue damage. Cellular activity plays a crucial role in the healing process, leading to a complex cascade. The wound's tensile power will be restored, resurfaced, and rebuilt after this activity²⁰. The development of wound tensile strength is equally important as preventing keloid formation²¹. The aim of medical and surgical practices is to heal incision wounds with no scars left. The process of wound healing has been accelerated and optimized by the creation and use of numerous aids and modern dressings^{3, 5, 8, 22}. BMMSC preparations that contain biological factors had a positive impact on collagen production and pain in burn patients, according to a recent study²³. Aram et al. using a different method, examined the use of 8% stem cell suspensions in empirical incisional wound models and noticed a decrease in inflammation and a reduction in wound size. The amount of collagen increased, and wound healing was accelerated due to no ulcerations.²⁴ During the current training, BMMSCs were better than saline when consumed during a dorsal graft-induced trauma curing classic. The preservation of rats by BMMSCs prevented hair root deterioration, and the epidermal thickness and amount of vessels, important data for repairing damage, were significantly higher than those of saline and control groups. The thickness of the epidermis can indicate the development of scars. The thinner the epidermis is, the greater the chance of scarring^{3, 25}. Epidermal thickness was greater in rats treated with BMMSCs. BMMSCs' increased fibroblast activity may have led to an acceleration of the epidermal healing process because of the optimization of collagen synthesis. In the cell group rats, there was a significant decrease in the percentage of necrotic tissue around the incision areas compared to the saline and control operated groups. Indicating that BMMSCs prevent necrosis, possibly through the inhibition of lipid peroxidation

in the tissues. The determination of biomechanical parameters was made. The analyses conducted on day 7 revealed no significant differences between the cell and pair groups in terms of Energy Absorption, Maximal Force, Ultimate Tensile Strength, and Bending Stiffness. The ultimate tensile strength and Bending stiffness are being recorded by all study groups. Collagen generation by macrophages. Although the possibility of direct macrophage collagen production via alternative activation was proposed more than 2 decades ago. Most scientists still reject it, particularly in wound healing. The primary process for healing incisional wounds involves the re-creation of mechanical strength by restoring tissue continuity.

The healing process is similar to excisional wounds, but they have a different physiological approach to the healing process. Intervention is necessary for excisional wound closure to form granulation tissue through angiogenesis and epithelialization. Conversely, the healing of surgical incision wounds is influenced more by the qualitative and quantitative formation of the extracellular matrix. The decrease in mechanical strength during wound healing studies plays a crucial role in preventing scar tissue formation^{16, 18, 20}. Disruption of vascular integrity is the cause of additional tissue damage and edema after incision injuries. Protease and reactive oxygen species (ROS) are produced by cells in the wound area to eliminate infection and cellular debris during the initial neutrophil infiltration into tissue during the inflammation phase⁴. To correct tissue ischemia, wound healing requires sufficient circulation³. Angiogenesis is associated with an increase in oxygen levels and a promotion of collagen synthesis and cell proliferation²⁶. In terms of vascularization, BMMSCs have been shown to have beneficial effects. Sections taken from rats treated with BMMSCs showed a significant increase in vascularization compared to the other groups. The histopathological examination in this study explored the effects of BMMSCs on wound healing by applying a dorsal skin flap model directly to the incision area. The BMMSCs group sections were found to have a similar distribution of collagen, scar formation, and discoloration to the intact skin. According to these findings, BMMSCs have beneficial effects on wound healing. In the BMMSCs group, collagen discoloration, an

essential measure of wound healing, was restricted and did not extend to the deeper areas of the dermis from the epidermal layer. The control and saline groups that did not receive cells saw an increase in collagen discoloration. The collagen was shown to be in a more effective form and in a structure that supported connective tissue formation by Trichrome Masson staining (Figure 2). Motta et al. properly modulated collagen lysis was revealed to lead to healthier fibroblast proliferation²⁶. Increased collagen synthesis could explain the optimization of collagen used in the BMMSCs group²⁷. As the last item, the decrease observed in the BMMSCs group in terms of collagen production might be caused by increased scavenger activity. It was used more effectively in connective tissue formation (Figure 2) because of the collagen-optimized fibroblast activity²⁶, and an image supporting the connective tissue formation emerged. The wound site in mice was found to have surprising hair growth after MSC-CM was injected subcutaneously around a full-thickness wound, as revealed by a study²⁷. The use of MSC-CM for hair follicle regeneration and wound healing is still in its infancy, particularly when using human hair follicle mesenchymal stem cells (HFMSCs) as the primary source. Despite HFMSCs being shown to have the potential for hair regrowth, it is necessary to identify the culture conditions that stimulate hair stimulating factors that merit this application. Therefore, clarifying the potential for regeneration of MSC-CM. We found that the BMMSCs group had a greater number of hair roots that were still intact in and around the incision area. The number of hair roots in the BMMSC group was greater than that of the other groups of incision. The BMMSCs group had a higher number of hair roots observed in the histological examination. BMMSCs application resulted in the *m. erector pili* near the hair roots being protected against oxidative stress. For this reason, the muscle condition in the BMMSCs group resembled that of the Control group more than the other incision groups.

According to all of these biomechanical tests, BMMSCs prevent the effects of oxidative stress at the cellular level. BMMSCs have the potential to prevent oxidative stress and have a positive impact on wound healing. However, their potent anti-oxidative qualities may be the main reason why they have a positive effect on wound healing.

ACKNOWLEDGMENTS

This study with (ethical code: IR.LUMS.REC.1397.111) was part of Maryam Habibi's dissertation (No. 958) M.Sc. With the support of Lorestan University of Medical Sciences (LUMS) Vice Chancellor for Research. Therefore, the authors are very grateful to LUMS.

Supplementary Materials

Supplementary file 1: manufacturer name, device name, device model and country of manufacture for histological and biomechanical analysis information. ([Materials in supplementary.docx](#))

CONFLICT OF INTEREST

The authors declare that there is no conflict of interests.

REFERENCES

1. Tsala DE, Habtemariam S, Simplicie FH, Thierry BNM, Abraham JA, Theophile D. Topically applied Tetrapleura tetraptera stem-bark extract promotes healing of excision and incision wounds in rats. *Journal of Intercult Ethnopharmacol* 2014;3(2):63.
2. Otimanam H, Tologbonse AA, Onwuka NA, Usen W. Cutaneous wound healing activity of herbal ointment containing Tetrapleura tetraptera fruit extract. *Nigerian J Pharmaceut Appl Sci Res* 2020;9(2):1-7.
3. Velnar T, Bailey T, Smrkolj V. The wound healing process: an overview of the cellular and molecular mechanisms. *J Int Med Res* 2009;37(5):1528-42.
4. Roy K, Shivakumar H, Sarkar S. Wound healing potential of leaf extracts of Ficus religiosa on Wistar albino strain rats. *Int J Pharm Tech Res* 2009;1:506-8.
5. Nayak B, Pinto Pereira LM. Catharanthus roseus flower extract has wound-healing activity in Sprague Dawley rats. *BMC Complementary and Alternative Medicine* 2006;6(1):1-6.
6. Pacheco NR, Pinto NdCC, Mello da Silva J, et al. Cecropia pachystachya: a species with expressive in vivo topical anti-inflammatory and in vitro antioxidant effects. *BioMed Res Int* 2014;2014.
7. Goorani S, Zangeneh MM, Koohi MK, et al. Assessment of antioxidant and cutaneous wound healing effects of Falcaria vulgaris aqueous extract in Wistar male rats. *Comparative Clin Pathol* 2019;28(2):435-45.
8. Hu MS, Borrelli MR, Lorenz HP, Longaker MT,

- Wan DC. Mesenchymal stromal cells and cutaneous wound healing: a comprehensive review of the background, role, and therapeutic potential. *Stem Cells International* 2018;**2018**.
9. Samy RP, Gopalakrishnakone P, Sarumathi M, Ignacimuthu S. Wound healing potential of *Tragia involucrata* extract in rats. *Fitoterapia* 2006;**77**(4):300-2.
 10. Kundu SC, Dash BC, Dash R, Kaplan DL. Natural protective glue protein, sericin bioengineered by silkworms: potential for biomedical and biotechnological applications. *Progress in Polymer Science* 2008;**33**(10):998-1012.
 11. Zhaorigetu S, Sasaki M, Watanabe H, KATO N. Supplemental silk protein, sericin, suppresses colon tumorigenesis in 1, 2-dimethylhydrazine-treated mice by reducing oxidative stress and cell proliferation. *Biosci, Biotech Biochem* 2001;**65**(10):2181-6.
 12. Kooti W, Ghasemiboroon AAM, Harizi M, et al. Effect of compound cream, a mixture of honey, fish oil, *Hypericum perforatum* L. and *Achilea mille folium* L. on full thickness skin wound in rat. *Res Pharmaceut Sci* 2012;**7**(5):18.
 13. Weissman IL. Stem cells: units of development, units of regeneration, and units in evolution. *Cell* 2000;**100**(1):157-68.
 14. Hu H, Li-Chan EC, Wan L, Tian M, Pan S. The effect of high intensity ultrasonic pre-treatment on the properties of soybean protein isolate gel induced by calcium sulfate. *Food Hydrocolloids* 2013;**32**(2):303-11.
 15. Zhao C, Chu Z, Miao Z, et al. Ultrasound heat treatment effects on structure and acid-induced cold set gel properties of soybean protein isolate. *Food Biosci* 2021;**39**:100827.
 16. Huang S, Xu L, Sun Y, Wu T, Wang K, Li G. An improved protocol for isolation and culture of mesenchymal stem cells from mouse bone marrow. *J Orthopaedic Translation* 2015;**3**(1):26-33.
 17. Ersel M, Uyanikgil Y, Akarca FK, et al. Effects of silk sericin on incision wound healing in a dorsal skin flap wound healing rat model. *Medical Science Monitor: International Medical Journal of Experimental and Clinical Research* 2016;**22**:1064.
 18. Masson-Meyers DS, Andrade TA, Caetano GF, et al. Experimental models and methods for cutaneous wound healing assessment. *Int J Exp Pathol* 2020;**101**(1-2):21-37.
 19. Edwards C, Marks R. Evaluation of biomechanical properties of human skin. *Clin Dermatol* 1995;**13**(4):375-80.
 20. Aramwit P, Kanokpanont S, Punyarit P, Srichana T. Effectiveness of inflammatory cytokines induced by sericin compared to sericin in combination with silver sulfadiazine cream on wound healing. *Wounds: A Compendium of Clinical Research and Practice* 2009;**21**(8):198-206.
 21. Sherman R, Rosenfeld H. Experience with the Nd: YAG laser in the treatment of keloid scars. *Ann Plast Surg* 1988;**21**(3):231-5.
 22. Sinno H, Malhotra M, Lutfy J, et al. Complements c3 and c5 individually and in combination increase early wound strength in a rat model of experimental wound healing. *Plast Surg Int* 2013;**2013**.
 23. Baoyong L, Jian Z, Denglong C, Min L. Evaluation of a new type of wound dressing made from recombinant spider silk protein using rat models. *Burns* 2010;**36**(6):891-6.
 24. Turan M, Ünver Saraydın S, Eray Bulut H, et al. Do vascular endothelial growth factor and basic fibroblast growth factor promote phenytoin's wound healing effect in rat? An immunohistochemical and histopathologic study. *Dermatol Surg* 2004;**30**(10):1303-9.
 25. Lee J-H, You H-J, Lee T-Y, Kang HJ. Current Status of Experimental Animal Skin Flap Models: Ischemic Preconditioning and Molecular Factors. *Int J Mol Sci* 2022;**23**(9):5234.
 26. Ramanathan G, Muthukumar T, Sivagnanam UT. In vivo efficiency of the collagen coated nanofibrous scaffold and their effect on growth factors and pro-inflammatory cytokines in wound healing. *Eur J Pharmacol* 2017;**814**:45-55.
 27. Siritienthong T, Ratanavaraporn J, Aramwit P. Development of ethyl alcohol-precipitated silk sericin/polyvinyl alcohol scaffolds for accelerated healing of full-thickness wounds. *Int J Pharmaceut* 2012;**439**(1-2):175-86.